RSC Advances

PAPER

View Article Online
View Journal | View Issue

Cite this: *RSC Adv.*, 2014, **4**, 27597

Biosynthesized Ag/α-Al_2O_3 catalyst for ethylene epoxidation: the influence of silver precursors

Xiaolian Jing,[a] Huixuan Wang,[a] Huimei Chen,[a] Jiale Huang,[a] Qingbiao Li[ab] and Daohua Sun*[a]

Received 12th April 2014
Accepted 9th June 2014

DOI: 10.1039/c4ra03312d

www.rsc.org/advances

Biosynthesized Ag/α-Al_2O_3 catalysts toward ethylene epoxidation were prepared with *Cinnamomum camphoratrees* (CC) extract using $AgNO_3$, silver–ammonia complex ($[Ag(NH_3)_2]^+$) and silver–ethylenediamine complex ($[Ag(en)_2]^+$) as the silver precursors. The catalyst from $[Ag(en)_2]^+$ demonstrated better activity compared to the catalysts from the other two precursors, 1.41% EO concentration with EO selectivity of 79.1% and 12.0% ethylene conversion were achieved at 250 °C. To investigate the influence of silver precursors on the catalytic performance, three catalysts were characterized by XRD, UV-Vis, XPS, SEM and O_2-TPD techniques. The results indicated that $[Ag(en)_2]^+$ precursors could be reduced more effectively by CC extract, and Ag particles were successfully immobilized onto the α-Al_2O_3 support under mild conditions. Moreover, a silver defects surface on the Ag/α-Al_2O_3 catalyst from $[Ag(en)_2]^+$ precursors had the best oxygen activation ability, playing an important role in the generation of electrophilic oxygen species which were responsible for the epoxidation reaction of C=C to EO.

Introduction

With the increasing environmental problems due to emissions of pollutants from the chemical industry, development of green synthesis of metal nanoparticles with various biological organisms in a more economical and eco-friendly mode has received more and more attention. Biosynthesis with the plant extract as both the reductant and stabilizing agent can successfully prepare and control the morphology of the metal nanoparticles in a simple way under mild conditions.[1,2] A series of plant extracts have been used to successfully synthesize Au,[3,4] Ag,[4–6] Pd,[7] Au–Ag[8,9] and Au–Pd[10] nanoparticles. For example, Au–Pd bimetallic nanoparticles were prepared based on simultaneous bioreduction of Au(III) and Pd(II) precursors with *Cacumen platycladi* (CP) leaf extract.[5] To date, the as-synthesized biogenic metal nanoparticles have been reported in many fields including optics,[11] antibacterial or antimicrobial agent,[2] biological control[12] and so on. Of special interest is that metal nanoparticles from plant extracts could also be used as catalyst which exhibited comparative or more excellent performance comparing with those from the conventional methods.[3,13–18] Reddy *et al.* reported that by using *Sapindus mukorossi* Gaertn fruit pericarp, gold nanoparticles from $HAuCl_4$ were obtained with good catalytic activity for the chemical reduction of *p*-nitroaniline.[3] Vilchis-Nestor *et al.* synthesized Au and AgAu nanostructures supported on SiO_2–Al_2O_3 by *C. sinensis* extract, the obtained catalysts possessed high catalytic performance and stability in oxidation and hydrogenation of CO.[13] Recent years, our group has also made great efforts on the preparation of catalysts with plant extracts.[14–18] It is found that bioreduction methods are easy to incorporate metal nanoparticles into supports under mild conditions. Besides, with plant biomass playing as both reductant and stabilizer, bioreduction could prepare metal particles with a narrower size distribution and a desired diameter, which is very important for the catalytic activity. Highly stable and active Au nanocatalyst toward propylene epoxidation was prepared through immobilizing biosynthesized Au nanoparticles onto TS-1 support and achieved excellent catalytic performance,[14,15] demonstrating the advantage of plant extract in fabrication of supported metal catalysts.

Ethylene oxide (EO) is vital chemical intermediate with diverse applications, the main method for producing EO is by the direct oxidation of ethylene with air or oxygen over a silver-based α-alumina catalyst.[19–21] Great interests have been focused on developing and optimizing the catalyst for more effective selectivity of EO due to both economic and technical reasons.[22] Conventionally, the Ag catalyst for ethylene epoxidation is prepared by impregnation through thermal decomposition process, in which silver nitrate[20] was the most common Ag precursors. Besides, Ag_2O,[23] silver lactate[24] and silver oxalate–ethylenediamine complex[25] were also employed. The catalysts prepared from different precursors showed varied properties closely related to their activities such as the oxygen adsorption and activation ability, Ag particle size and distribution on the support *etc.*

[a]*Department of Chemical and Biochemical Engineering, and National Laboratory for Green Chemical Productions of Alcohols, Ethers and Esters, College of Chemistry and Chemical Engineering, Xiamen University, Xiamen, 361005, P. R. China. E-mail: sdaohua@xmu.edu.cn; Fax: +86 592-2184822; Tel: +86 592-2183088*
[b]*Quanzhou Normal University, Quanzhou, 362002, P. R. China*

Very recently, we reported that biomass in *Cinnamomum camphoratrees* (CC) extract could reduce sintering during the thermal decomposition process.[18] In the present work, the catalytic performance of silver catalysts was obviously enhanced by replacing silver nitrate with other silver precursors. To clarify the influence of silver precursors on the structure, surface state, oxidation property thus ethylene epoxidation reaction activity, a simple impregnation–bioreduction method with CC extract was used to prepare Ag/α-Al_2O_3 catalysts from three different Ag precursors, *i.e.* $AgNO_3$, silver–ammonia complex ($[Ag(NH_3)_2]^+$) and silver–ethylenediamine complex ($[Ag(en)_2]^+$) for ethylene epoxidation reaction. X-ray powder diffraction (XRD), UV-Vis DRS, X-ray photoelectron spectra (XPS), Scanning electron microscopic (SEM) as well as O_2-temperature-programmed desorption (O_2-TPD) were employed for the characterizations.

Experimental

Materials

$AgNO_3$ (A.R.), ethylenediamine (A.R.) and ammonium hydroxide (A.R.) were purchased from Sinopharm Chemical Reagent Co. Ltd., China. α-Al_2O_3 was supplied by Tianjin Chemical Research & Design Institute. *Cinnamomum camphoratrees* leaves were picked up in Xiamen University.

Silver–ammonia complex ($[Ag(NH_3)_2]^+$) was prepared by continuously dropping ammonium hydroxide into the $AgNO_3$ solution until the firstly formed precipitate dissolved and the solution becomes clear. Silver–ethylenediamine complex ($[Ag(en)_2]^+$) was also prepared from $AgNO_3$ as following: ammonium oxalate solution was added into $AgNO_3$ solution and the white precipitate was obtained. After filtering and washing with deionized water, the precipitate was dried in vacuum and dissolved in a mixture of water and ethylenediamine (1 : 1, v/v) to obtain the required complex solution. Ag concentration is 1.36 M in both silver–ammonia complex and silver–ethylenediamine complex solution.

Preparation of Ag/Al_2O_3 catalysts

Preparation of CC extract: the fresh CC leaves were washed and completely dried. Then, the dried leaves were milled and screened with a 20-mesh sieve. 15 g powder was added to 100 mL deionized water and the mixture was shaken at 30 °C for 12 h with a rotation rate of 150 rpm. After that, the solution was filtered and proper amount of deionized water was added to keep the volume of the filtrate at 100 mL. The concentration of the CC extract was denoted as 15 g L^{-1}.

Preparation of Ag/α-Al_2O_3 catalyst: the catalyst was prepared by an impregnation–bioreduction process with three different Ag precursors, namely, $AgNO_3$, silver–ammonia complex and silver–ethylenediamine complex (concentration of Ag in different precursors is 1.36 M). Firstly, the industrial α-Al_2O_3 was crushed, size of 20–40 mesh was collected and calcined at 600 °C for 6 h. The pretreated α-Al_2O_3 support (1.0 g) was impregnated with silver precursors (1.2 mL), and dried at 50 °C for 12 h in vacuum. Then the obtained solid was dipping with CC extract in an iso volumetric way for 24 h at 60 °C. Afterwards, the catalyst was dried at 50 °C for 24 h in vacuum. The theoretical loading amount of Ag was 15 wt% in the obtained catalysts from different silver precursors. The catalyst samples are denoted as Ag/α-Al_2O_3-x, where x represents the Ag precursors (the $AgNO_3$, Ag-ammonia complex and Ag–ethylenediamine complex precursors are designated as n, a, and en, respectively).

Characterization techniques

X-ray powder diffraction (XRD) patterns were obtained at room temperature with a Panalytical X'pert PRO diffractometer (PANalytical BV, Netherlands) with monochromatized CuKα radiation at a voltage of 40 kV and a current of 30 mA. The ultraviolet-visible diffuse reflectance spectra (UV-Vis DRS) of the samples were collected on a Cary 5000 spectrophotometer (Varian, USA) with dehydrated $BaSO_4$ as the reference. X-ray photoelectron spectra (XPS) of the catalysts were obtained on a Quantum-2000 ESCA Microprobe spectrometer (PHI, USA) with an Al Ka (1486.6 eV) as the X-ray source and the results were calibrated internally by the carbon deposit C(1s) ($E_b = 284.6$ eV). Scanning electron microscopic (SEM) observations were carried out on a LEO-1530 Electron Microscope (LEO, Germany). The size distribution of the silver nanoparticles of the catalysts was estimated on the basis of several relative SEM micrographs using SigmaScan Pro software. O_2-temperature-programmed desorption (O_2-TPD) measurements were performed on a Micromeritics Auto Chem 2920 II instrument. Typically, 0.5 g sample was pretreated under a He flow of 30 mL min^{-1} at 250 °C for 1 h, then the sample was cooled down to 170 °C and switched to an O_2 flow of 30 mL min^{-1}. After 1 h, the sample were cooled down to room temperature and switched to a He flow to remove O_2 in gas phase. Then O_2 desorption was performed by heating the sample in He flow to 700 °C at a rate of 10 °C min^{-1}. The desorbed O_2 were detected using a thermal conductivity detector (TCD).

Catalytic activity measurements

Catalytic reactions were carried out in a vertical fixed-bed stainless-steel reactor at 2 MPa pressure. The feed gas was comprised of 15 vol% C_2H_4, 7 vol% O_2 and 5 vol% CO_2 balanced with N_2. 0.5 mL catalyst was used at a space velocity of 7000 mL h^{-1} mL_{cat}^{-1}. The gas leaving the reactor was heated at about 115 °C and analyzed online by a gas chromatograph. The chromatograph was equipped with a TCD, using a Porapak Q packed column (2 mm × 3 m), and a flame ionization detector (FID), using a β-β-oxydipropionitrile packed column (2 mm × 1.5 m).

Results and discussion

Ethylene epoxidation over the Ag/α-Al_2O_3 catalysts

The catalytic performance for ethylene epoxidation over the Ag/α-Al_2O_3 catalysts prepared from different silver precursors is shown in Fig. 1. It can be seen that the reaction activities of the three catalysts are very different from one another. For the ethylene epoxidation over the Ag/α-Al_2O_3-en catalyst, considerable EO concentration (0.82%) was achieved at the initial

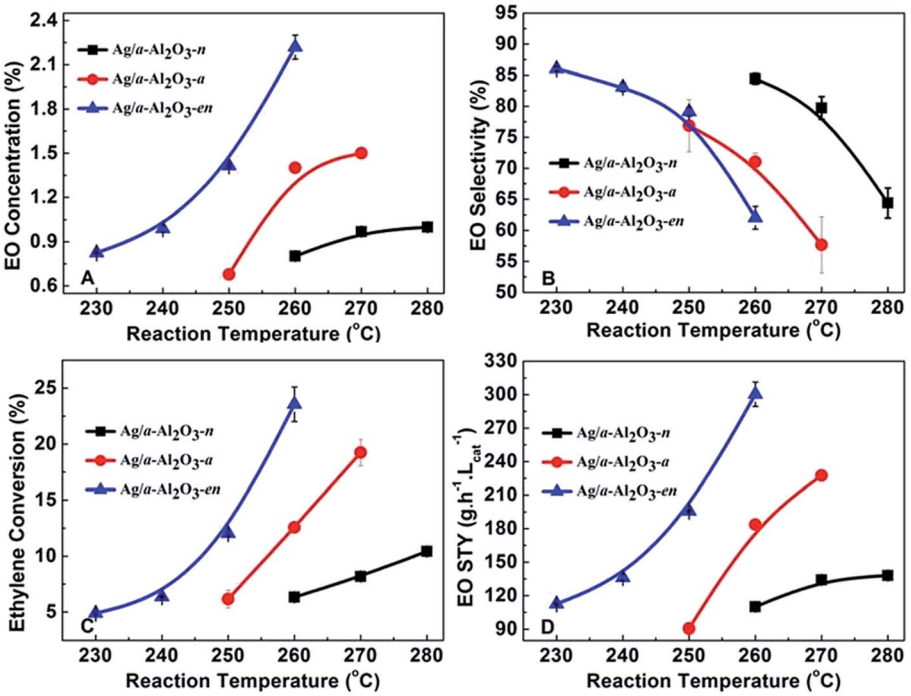

Fig. 1 Epoxidation of ethylene over Ag/α-Al_2O_3 catalysts prepared from different silver precursors. Reaction conditions: feed gas $V(C_2H_4) : V(O_2) : V(CO_2) : V(N_2) = 15 : 7 : 5 : 73$, reaction pressure = 2 MPa, GHSV = 7000 mL h^{-1} mL_{cat}^{-1}.

evaluation temperature 230 °C and with the increasing temperature, EO concentration increased obviously. EO concentration of 1.41% with EO selectivity of 79.1% and 12.0% ethylene conversion were achieved at 250 °C. The EO concentration further increased to 2.22% at 260 °C while the EO selectivity decreased to 62.03%. The performance of the catalysts prepared from $AgNO_3$ and silver–ammonia complex (Ag/α-Al_2O_3-n and Ag/α-Al_2O_3-a) was relatively lower than that of Ag/α-Al_2O_3-en at the same temperature. For the Ag/α-Al_2O_3-a catalyst, EO concentration increased from 0.67 to 1.50% and the selectivity decreased from 76.88 to 57.68% with the temperature increasing from 250 to 270 °C. For the ethylene epoxidation over Ag/α-Al_2O_3-n catalyst, lower EO concentration (≤1%) and ethylene conversion (6.33–10.43%) was shown between 260 and 280 °C.

Generally, more attentions are focused on controlling the EO selectivity rather than the ethylene conversion when the industrial requirement of EO concentration (1.30–1.50%) is reached. In order to compare the selectivity of different catalysts under the similar EO concentration in a more intuitive way, the EO selectivity against EO concentration over Ag/α-Al_2O_3 with different silver precursors is shown in Fig. 2. In the range of reaction temperature, the EO concentration of Ag/α-Al_2O_3-n (0.80–1%) did not achieve the industrial requirement of EO concentration, when increasing the reaction temperature, the EO selectivity declined rapidly from 84.43 to 64.40%. As to the Ag/α-Al_2O_3-a and Ag/α-Al_2O_3-en, both catalysts could reach the industrial requirement of EO concentration. Ag/α-Al_2O_3-en achieved 1.41% EO concentration at 250 °C with 79.11% EO selectivity, while for Ag/α-Al_2O_3-a catalyst, at 260 °C the comparable EO concentration could be reached with a lower selectivity of 71.04%. Hence, it could be concluded that the catalyst prepared from silver–ethylenediamine complex exhibited the best catalytic activity with 1.41% EO concentration, 79.1% EO selectivity and space time yield of 195.63 g h^{-1} L_{cat}^{-1} at 250 °C.

XRD and SEM analysis

Structure features of the obtained Ag/α-Al_2O_3 catalyst from three precursors were investigated using powder XRD characterization. The diffraction peaks of α-Al_2O_3 support locate at 2θ = 25.6, 35.2, 37.7, 43.4, 52.6, 57.5, 66.5 and 68.2°. Fig. 3A exhibits

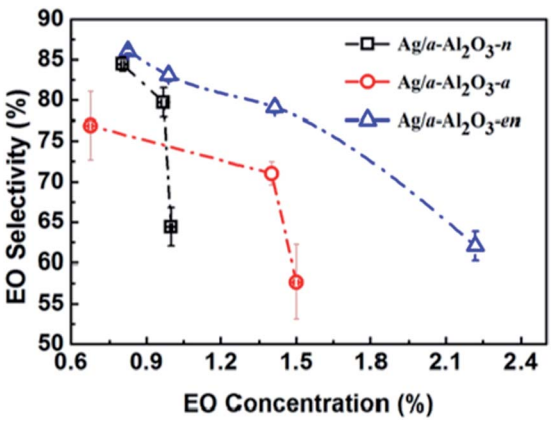

Fig. 2 The EO selectivity *versus* EO concentration over Ag/α-prepared from different silver precursors.

the XRD patterns of α-Al_2O_3 support impregnated with $AgNO_3$, $[Ag(NH_3)_2]^+$ and $[Ag(en)_2]^+$ without bioreduction. The results showed that only peaks of Ag precursors were found on the α-Al_2O_3 support, and no obvious diffraction peaks of metallic Ag emerged by impregnation with Ag salts. After dipping in CC extract for 24 h, shown in Fig. 3B, typical diffraction peaks of Ag emerged at $2\theta = 38.1$, 44.3, 64.4, 77.4 and 81.5°, corresponding to the crystal faces of Ag(111), (200), (220), (311) and (222), respectively. Though metallic Ag was successfully loaded onto the support by impregnation–bioreduction process, there were differences in the diffractions peaks of Ag/α-Al_2O_3 samples from different precursors. Fig. 3B inset shows more details of peaks of the samples. The peak intensity of metallic Ag (111) on these samples increased as follows: Ag/α-Al_2O_3-n < Ag/α-Al_2O_3-a < Ag/α-Al_2O_3-en. Besides, diffraction peaks of Ag precursors were also found on Ag/α-Al_2O_3-n and Ag/α-Al_2O_3-a samples (a′ and b′ curves in Fig. 3B) comparing with the corresponding curves in Fig. 3A. As to the Ag/α-Al_2O_3-en (c′ in Fig. 3B) sample, metallic Ag was found to be the only species in the catalysts. These results indicated that the impregnation–bioreduction method could effectively load silver onto the α-Al_2O_3 support in a mild way, and CC extract could reduce Ag^+, $[Ag(NH_3)_2]^+$ or $[Ag(en)_2]^+$ into metallic silver. For different Ag precursors, the degree of reduction was in the order as follows: Ag/α-Al_2O_3-en > Ag/α-Al_2O_3-a > Ag/α-Al_2O_3-n. Particularly, no obvious diffraction peaks related to silver precursor were detected on Ag/α-Al_2O_3-en catalyst.

SEM was used to observe the morphology of the supported Ag nanoparticles on α-Al_2O_3. Al_2O_3 is large flake-shape, while Ag particles (see arrows), much smaller and spherical are supported on it. A small quantity of Ag particles was found on Ag/α-Al_2O_3-n sample (Fig. 4A). Though more Ag were observed on Ag/α-Al_2O_3-a (Fig. 4B), Ag particles aggregated obviously and distributed unevenly as in Fig. 4A. With regard to the catalyst prepared from $[Ag(en)_2]^+$, large amount of Ag nanoparticles were well dispersed on the support (Fig. 4C) with a statistic diameter of 93.2 ± 41.2 nm (Fig. 4D).

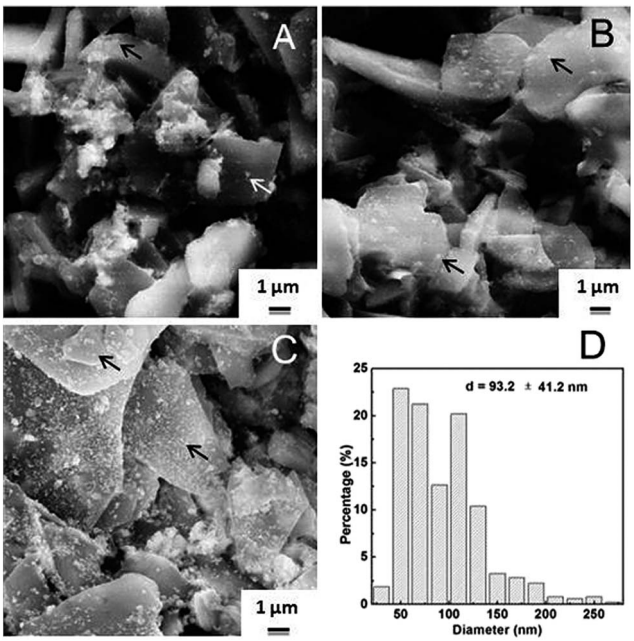

Fig. 4 SEM images of (A) Ag/α-Al_2O_3-n, (B) Ag/α-Al_2O_3-a and (C) Ag/α-Al_2O_3-en catalysts and (D) the corresponding histogram of size distribution of Ag particles on Ag/α-Al_2O_3-en. Arrows in (A)–(C) indicate the Ag nanoparticles on α-Al_2O_3 support.

UV-Vis DRS characterization

UV-Vis DRS was used to identify Ag oxidation state of the three catalysts. As shown in Fig. 5, obvious absorption band at

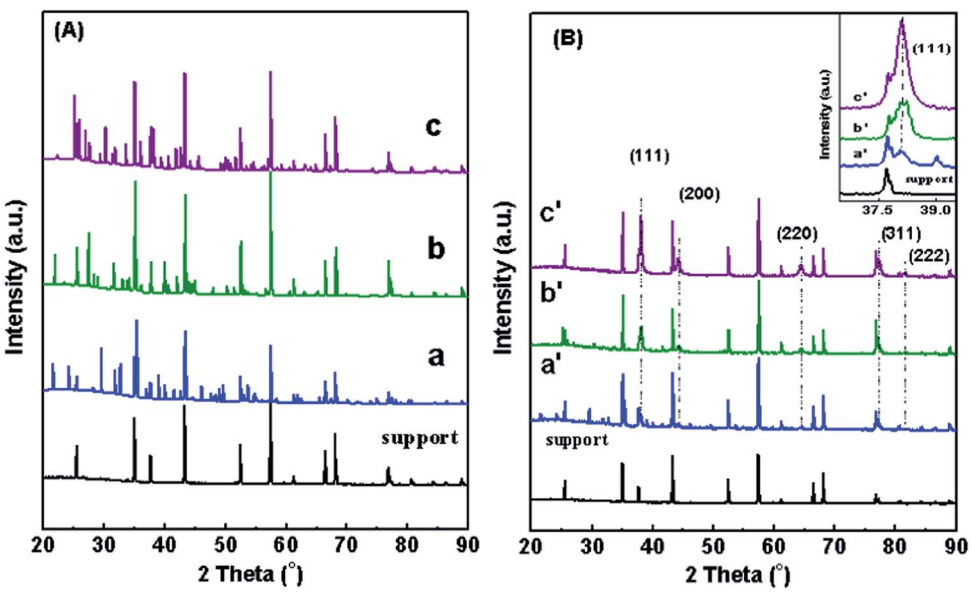

Fig. 3 (A) XRD patterns of α-Al_2O_3 support impregnated with (a) $AgNO_3$, (b) $[Ag(NH_3)_2]^+$ and (c) $[Ag(en)_2]^+$; (B) XRD patterns of (a′) Ag/α-Al_2O_3-n, (b′) Ag/α-Al_2O_3-a and (c′) Ag/α-Al_2O_3-en catalysts.

~200 nm aroused by the electron transition of $4d^{10}$–$4d^{9}5s^{1}$ from the highly dispersed Ag^{+} on the support,[26] emerged on both Ag/α-Al_2O_3-n and Ag/α-Al_2O_3-a catalysts, indicating that $AgNO_3$ and $[Ag(NH_3)_2]^{+}$ precursors were not reduced completely. Absorption band at 250–260 nm, attributed to the electron transition of $4d^{10}5s^{1}$–$4d^{9}5s^{1}5p^{1}$, $4d^{10}5s^{1}$–$4d^{9}5s^{1}6p^{1}$ or $5s^{1}$–$5p^{1}$ from metallic Ag,[27–29] was observed on the three catalyst, indicating the existence of Ag^{0} on them. Ag/α-Al_2O_3-en catalyst (Fig. 5c) had the strongest band intensity of ~250 nm compared with the other two samples, suggesting that more metallic Ag existed on this sample. Bands at the 296 nm and 350 nm assigned to the $Ag_n^{\delta+}$ clusters, which were formed by the interaction between metallic silver and the support, could promote the reaction of ethylene epoxidation.[30–34] Comparing with the other two, band at 296 nm is stronger of Ag/α-Al_2O_3-en which exhibiting the best catalytic activity of ethylene epoxidation. UV-Vis DRS analysis also indicated that by impregnation–bioreduction process with CC extract, silver oxidation state from different precursors on the same support was different. Though CC extract could reduce the three precursors to Ag^{0}, obvious Ag^{+} (~200 nm) was detected on the catalyst surface for Ag/α-Al_2O_3-n and Ag/α-Al_2O_3-a, while for Ag/α-Al_2O_3-en, no obvious band of Ag^{+} emerged. It could be concluded that CC completely reduced the $[Ag(en)_2]^{+}$ precursor.

XPS analysis

XPS experiment was performed in order to get more information about the electronic states of Ag on the three catalysts prepared from different precursors. As shown in Fig. 6, two bands of Ag $3d_{5/2}$ were observed at 367.2 and 368.1–368.7 eV. The former band (367.2 eV) is assigned to the metallic Ag^{0} particles[19,35] and the latter (368.1–368.7 eV) is associated with the presence of high oxidation valence state $Ag^{\delta+}$ species.[43–45] Generally the binding energy of metallic Ag $3d_{5/2}$ is at 367.9 eV.[36,37] Fig. 6 shows that the peak shifts obviously to lower binding energy, which was attributed to the differential charging effect aroused by the interaction between Ag and the support.[35] XPS spectra in Fig. 6 also exhibited the three catalysts had different ratios of Ag^{0} and $Ag^{\delta+}$: Ag species on Ag/α-Al_2O_3-n catalyst had a high concentration of $Ag^{\delta+}$ while on Ag/α-Al_2O_3-en, there was mainly Ag^{0} species. The valence distributions of Ag of different Ag/α-Al_2O_3 catalysts are presented in Table 1. It could be clearly seen that Ag precursors had significant effects on the electronic state of Ag on the catalysts. The percentage of metallic Ag were 78.64, 48.16 and 27.21% on the catalysts from $AgNO_3$, $[Ag(NH_3)_2]^{+}$ and $[Ag(en)_2]^{+}$, respectively. And it should be noted that, based on the results of XRD (Fig. 3) and UV-Vis DRS (Fig. 5), $Ag^{\delta+}$ on Ag/α-Al_2O_3-n and Ag/α-Al_2O_3-a catalysts originated from the incompletely reduced precursors and the $Ag_n^{\delta+}$ clusters formed by the interaction between metallic silver and the support, while for Ag/α-Al_2O_3-en sample, $Ag^{\delta+}$ were mainly the $Ag_n^{\delta+}$ clusters.

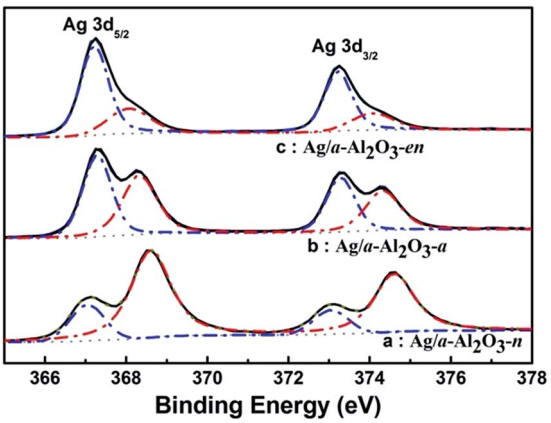

Fig. 6 XPS spectra of Ag 3d regions recorded on (a) Ag/α-Al_2O_3-n, (b) Ag/α-Al_2O_3-a and (c) Ag/α-Al_2O_3-en catalysts.

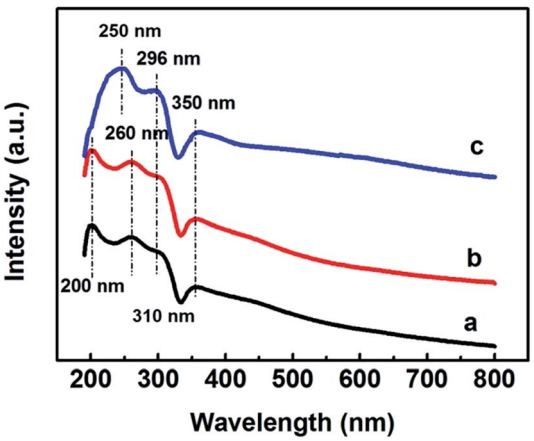

Fig. 5 UV-Vis DRS spectra of (a) Ag/α-Al_2O_3-n, (b) Ag/α-Al_2O_3-a and (c) Ag/α-Al_2O_3-en catalysts.

O_2-TPD analysis

Oxygen activation on the catalyst surface plays an important role in ethylene epoxidation reaction, and O_2-TPD is one of the most effective techniques to study the oxygen adsorption and activation ability of the catalysts.[38,39] Molecularly adsorbed O_2 species desorbs from Ag at a relatively low temperature[40] while desorption of lattice oxygen occurs at above 750 °C,[41] and it is generally believed that the atomic oxygen which desorbs at 200–500 °C is the reactive species on silver catalysts.[38] Fig. 7 shows the O_2-TPD characterizations of the three catalysts. Based on the corresponding area of the peaks between 200 and 500 °C, the ratio of desorbed O_2 was 1(Ag/α-Al_2O_3-n):1.5 (Ag/α-Al_2O_3-a): 7.21 (Ag/α-Al_2O_3-en), indicating that Ag/α-Al_2O_3-en catalyst had a stronger oxygen adsorption ability. Note that two shoulder peaks emerged at 248 and 403 °C in addition to the main one at 323 °C for the Ag/α-Al_2O_3-en catalyst (Fig. 7c), the peak at 248 °C could be attributed to the nucleophilic oxygen species desorbing from regular surface and the peak at 323 °C to electrophilic oxygen species desorbing from imperfect or defect regions of the silver surface.[42–44] The desorption peak at 403 °C was referred to oxygen species desorbing from the subsurface of silver.[45] And it was believed that nucleophilic oxygen species located on the regular surface of silver was responsible for promoting the adsorption of C_2H_4 on Ag surface,[21] and the

Table 1 Valence distribution of Ag on Ag/α-Al_2O_3 catalysts prepared from different silver precursors

	Ag^0		$Ag^{\delta+}$	
Catalyst	BE (Ag $3d_{5/2}$) (eV)	Percentage (%)	BE(Ag $3d_{5/2}$) (eV)	Percentage (%)
Ag/α-Al_2O_3-n	367.1	21.36	368.6	78.64
Ag/α-Al_2O_3-a	367.3	51.84	368.3	48.16
Ag/α-Al_2O_3-en	367.2	72.79	368.1	27.21

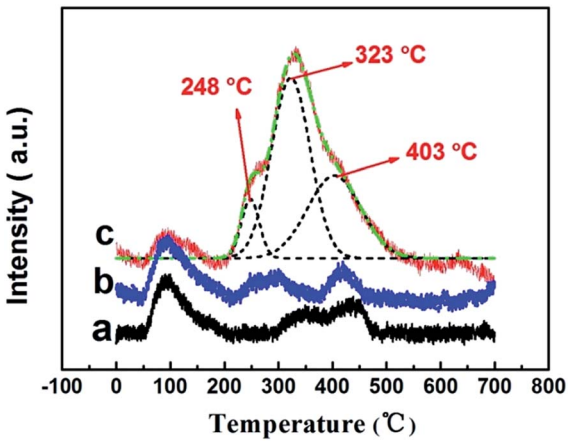

Fig. 7 O_2-TPD profiles of Ag/α-Al_2O_3 prepared from different silver precursors: (a) Ag/α-Al_2O_3-n, (b) Ag/α-Al_2O_3-a and (c) Ag/α-Al_2O_3-en.

electrophilic oxygen species adsorbed on the silver defects surface could attack the carbon–carbon double bond of ethylene to produce EO.[42] Thus, O_2-TPD results also clarified the catalyst prepared from $Ag[(en)_2]^+$ with CC extract had the best reaction activity due to the excellent oxygen activation ability.

Conclusions

In summary, we have reported the synthesis of α-Al_2O_3 supported silver catalysts for ethylene epoxidation through an impregnation–bioreduction process using CC extract. Comparative studies were carried out among three catalysts prepared with different Ag precursors, namely $AgNO_3$, $[Ag(NH_3)_2]^+$ and $[Ag(en)_2]^+$. It was found that the Ag/α-Al_2O_3-en catalyst exhibited higher catalytic activity than the other two ones. EO concentration of 1.41% with EO selectivity of 79.1% and 12.0% ethylene conversion were achieved at 250 °C over Ag/α-Al_2O_3-en catalyst, and SEM images indicated that large amount of Ag nanoparticles were well dispersed on the support with a statistic diameter of 93.2 ± 41.2 nm. XRD, UV-Vis, XPS characterization results indicated that $[Ag(en)_2]^+$ precursor was reduced more thoroughly by CC extract when comparing with the other two Ag precursors. The degree of reduction by the CC extract was in the order as follows: Ag/α-Al_2O_3-en > Ag/α-Al_2O_3-a > Ag/α-Al_2O_3-n. O_2-TPD analysis suggested that silver defects surface on Ag/α-Al_2O_3-en catalyst formed by the impregnation–bioreduction using CC extract with $Ag[(en)_2]^+$ had the best oxygen activation ability, which plays an important role in ethylene epoxidation reaction.

Acknowledgements

This work was supported by the NSFC Projects (nos. 21206140 and 21036004) and the fund of the State Key Laboratory of Advanced Technologies for Comprehensive Utilization of Platinum Metals (SKL-SPM-201210).

Notes and references

1 S. S. Shankar, A. Rai, A. Ahmad and M. Sastry, *J. Colloid Interface Sci.*, 2004, **275**, 496–502.
2 A. K. Mittal, Y. Chisti and U. C. Banerjee, *Biotechnol. Adv.*, 2013, **31**, 346–356.
3 V. Reddy, R. S. Torati, S. Oh and C. Kim, *Ind. Eng. Chem. Res.*, 2012, **52**, 556–564.
4 J. Huang, Q. Li, D. Sun, Y. Lu, Y. Su, X. Yang, H. Wang, Y. Wang, W. Shao and N. He, *Nanotechnology*, 2007, **18**, 105104.
5 J. Huang, L. Lin, Q. Li, D. Sun, Y. Wang, Y. Lu, N. He, K. Yang, X. Yang and H. Wang, *Ind. Eng. Chem. Res.*, 2008, **47**, 6081–6090.
6 S. Yudha, S. D. Notriawan, E. Angasa, T. Eka Suharto, J. Hendri and Y. Nishina, *Mater. Lett.*, 2013, **97**, 181–183.
7 X. Yang, Q. Li, H. Wang, J. Huang, L. Lin, W. Wang, D. Sun, Y. Su, J. B. Opiyo and L. Hong, *J. Nanopart. Res.*, 2010, **12**, 1589–1598.
8 A. A. AbdelHamid, M. A. Al-Ghobashy, M. Fawzy, M. B. Mohamed and M. M. Abdel-Mottaleb, *ACS Sustainable Chem. Eng.*, 2013, **1**, 1520–1529.
9 N. M. Nori, K. Abdi, M. R. Khoshayand, S. H. Ahmadi, N. Lamei and A. R. Shahverdi, *J. Exp. Nanosci.*, 2012, **8**, 442–450.
10 G. Zhan, J. Huang, M. Du, I. Abdul-Rauf, Y. Ma and Q. Li, *Mater. Lett.*, 2011, **65**, 2989–2991.
11 A. Ravindran, P. Chandran and S. S. Khan, *Colloids Surf., B*, 2013, **105**, 342–352.
12 N. K. Mondal, A. Chowdhury, U. Dey, P. Mukhopadhya, S. Chatterjee, K. Das and J. K. Datta, *Asian Pac. J. Trop. Dis.*, 2014, **4**, S204–S210.
13 A. Vilchis-Nestor, M. Avalos-Borja, S. Gómez, J. A. Hernández, A. Olivas and T. Zepeda, *Appl. Catal., B*, 2009, **90**, 64–73.

14 G. Zhan, M. Du, J. Huang and Q. Li, *Catal. Commun.*, 2011, **12**, 830–833.
15 M. Du, G. Zhan, X. Yang, H. Wang, W. Lin, Y. Zhou, J. Zhu, L. Lin, J. Huang and D. Sun, *J. Catal.*, 2011, **283**, 192–201.
16 G. Zhan, Y. Hong, V. T. Mbah, J. Huang, A.-R. Ibrahim, M. Du and Q. Li, *Appl. Catal., A*, 2012, **439–440**, 179–186.
17 J. Huang, C. Liu, D. Sun, Y. Hong, M. Du, T. Odoom-Wubah, W. Fang and Q. Li, *Chem. Eng. J.*, 2014, **235**, 215–223.
18 D. Sun, H. Wang, G. Zhang, J. Huang and Q. Li, *RSC Adv.*, 2013, **3**, 20732–20737.
19 D. M. Minahan, G. B. Hoflund, W. S. Epling and D. W. Schoenfeld, *J. Catal.*, 1997, **168**, 393–399.
20 J. T. Jankowiak and M. A. Barteau, *J. Catal.*, 2005, **236**, 366–378.
21 V. Bukhtiyarov, A. Carley, L. Dollard and M. Roberts, *Surf. Sci.*, 1997, **381**, L605–L608.
22 C. Stegelmann, N. C. Schiødt, C. T. Campbell and P. Stoltze, *J. Catal.*, 2004, **221**, 630–649.
23 J. Lu, J. J. Bravo-Suárez, A. Takahashi, M. Haruta and S. T. Oyama, *J. Catal.*, 2005, **232**, 85–95.
24 M. C. N. Amorim de Carvalho, F. B. Passos and M. Schmal, *J. Catal.*, 2007, **248**, 124–129.
25 N. Macleod, J. M. Keel and R. M. Lambert, *Catal. Lett.*, 2003, **86**, 51–56.
26 J. Texter, J. J. Hastreiter and J. L. Hall, *J. Phys. Chem.*, 1983, **87**, 4690–4693.
27 V. I. Srdanov and D. S. Pešić, *J. Mol. Spectrosc.*, 1981, **90**, 27–32.
28 C. Steinbrüchel and D. Gruen, *Surf. Sci.*, 1981, **106**, 160–164.
29 G. A. Ozin and H. Huber, *Inorg. Chem.*, 1978, **17**, 155–163.
30 K. A. Bethke and H. H. Kung, *J. Catal.*, 1997, **172**, 93–102.
31 L. Kundakovic and M. Flytzani-Stephanopoulos, *Appl. Catal., A*, 1999, **183**, 35–51.
32 A. Pestryakov and A. Davydov, *J. Electron Spectrosc. Relat. Phenom.*, 1995, **74**, 195–199.
33 A. Keshavaraja, X. She and M. Flytzani-Stephanopoulos, *Appl. Catal., B*, 2000, **27**, L1–L9.
34 X. She and M. Flytzani-Stephanopoulos, *J. Catal.*, 2006, **237**, 79–93.
35 Y. Xu, H. Xu, H. Li, J. Xia, C. Liu and L. Liu, *J. Alloys Compd.*, 2011, **509**, 3286–3292.
36 G. Jin, G. Lu, Y. Guo, Y. Guo, J. Wang and X. Liu, *Catal. Lett.*, 2003, **87**, 249–252.
37 W. Yao, Y. L. Guo, X. H. Liu, Y. Guo, Y. Q. Wang, Y. S. Wang, Z. G. Zhang and G. Z. Lu, *Catal. Lett.*, 2007, **119**, 185–190.
38 J. Serafin, A. Liu and S. Seyedmonir, *J. Mol. Catal. A: Chem.*, 1998, **131**, 157–168.
39 G. Busser, O. Hinrichsen and M. Muhler, *Catal. Lett.*, 2002, **79**, 49–54.
40 C. T. Campbell, *Surf. Sci.*, 1985, **157**, 43–60.
41 Y.-C. Kim, N.-C. Park, J.-S. Shin, S. R. Lee, Y. J. Lee and D. J. Moon, *Catal. Today*, 2003, **87**, 153–162.
42 B. Bal'zhinimaev, *Kinet. Catal.*, 1999, **40**, 795–810.
43 J. Couves, M. Atkins, M. Hague, B. Sakakini and K. Waugh, *Catal. Lett.*, 2005, **99**, 45–53.
44 J. C. Dellamorte, J. Lauterbach and M. A. Barteau, *Top. Catal.*, 2010, **53**, 13–18.
45 M. C. Amorim de Carvalho, F. B. Passos and M. Schmal, *J. Catal.*, 2007, **248**, 124–129.